JOURNAL OF MATERIALS SCIENCE 20 (1985) 3400 – 3408

A new type of fatigue striation on PMMA immersed in organic agents

M. KITAGAWA, H. KANZAKI
Department of Mechanical Engineering, Faculty of Technology, Kanazawa University, 2-40-20 Kodatsuno, Kanazawa, Japan

Fatigue crack growth tests of PMMA were undertaken at 295 K in organic agents with relatively high viscosity. Regular wavy striations, the wave length and amplitude of which were dependent on the characteristics of the agent, appeared on the fracture surfaces at low values of the stress intensity factor ranges. This type of striation has not been reported elsewhere. The formation mechanism of these was analysed based on the two dimensional viscous-fluid flow through a narrow gap between the crack planes. The theoretical suggestion that the wave length of the striation tends to increase with increase in the surface tension of the liquid and a decrease in its viscosity was in good agreement with the experimental trend.

1. Introduction

The crack growth behaviour of poly(methyl methacrylate) (PMMA) was investigated under creep, quasi-static and fatigue loading conditions in some environments [1–5]. From these results, it has been found that fracture mechanics parameters such as stress intensity factor and strain energy release rate are important for understanding the mechanism of the crack growth. However, there does not seem to exist any theory which explains those cracking behaviours at the same time. For this reason, we intended to derive a criterion to express the cracking behaviour by the use of only material constants such as creep compliance and structural units to be measured by means of simple material tests. As a link in the chain of this work, the tests under cyclic loading were performed in some organic agents with relatively high viscosity. The fracture surface of the first test sample immersed in propylene glycol was observed through an optical microscope and was found to be covered with regular wavy striations somewhat different from those usually observed. It seems that these striations have not been reported elsewhere and, probably, are of a new type.

The purpose of this paper, therefore, is to provide experimental evidence of this new type of striation and to discuss their formation mechanism. Then, fatigue crack growth experiments were performed in organic agents with various values of viscosity and surface tension using compact tension specimens.

2. Experimental details

The material used was PMMA plate (Kanase Co, Japan) 5 mm thick. Compact tension (CT) specimens, the dimensions of which are indicated in Fig. 1, were machined from them. Their dimensions were geometrically similar to those of the ASTM standard [6] except for their thickness. The milled crack starter cut perpendicular to the tensile direction was subjected to cyclic loading to form a natural crack.

The fatigue tests were carried out at zero-tension loading in a chamber filled with viscous organic agents, as schematically illustrated in Fig. 1. The organic agents used are listed in Table I, which includes the values of their viscosity and surface tension and the symbols marked in the figures. These are known to be crazing agents. If as-machined specimens were pulled in the agents used, numerous large crazes nucleate on both sides of the specimen surface near the crack tip. Then, to prevent their

0022–2461/85 $03.00 + .12

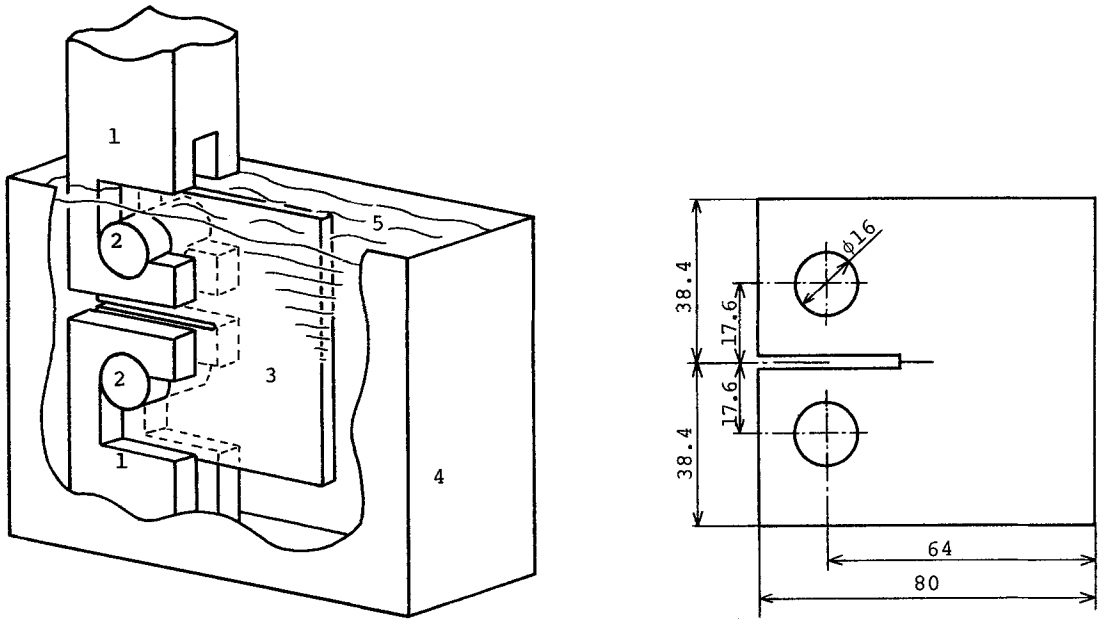

Figure 1 Illustration of testing apparatus and specimen dimensions. 1, tensile jigs; 2, loading pins; 3, specimen; 4, chamber; 5, organic agent.

initiation, a part of both surfaces was thinly (less than 10^{-5} m) covered along the direction of crack growth with epoxy resin (Araldite). The maximum and the minimum loads were kept constant during the test. The loading frequency was in the range 0.1 to 2.5 Hz, and the test temperature was 298 K. The length of crack was measured by a travelling microscope without stopping the test. The macroscopic crack growth rates were determined from the tangents of a crack length–cycles diagram. The stress intensity factor range (ΔK) was calculated from the equation usually used for the CT specimen [6]. Fracture surfaces were observed by an optical microscope.

TABLE I Viscosity and surface tension of the organic agents at 25° C

Organic agent	Viscosity (cP)	Surface tension (dyne cm^{-1})	Symbol
Propylene glycol (PG)	43	34	○
Ethylene glycol (EG)	17	44	▽
Diethlene glycol (DG)	28	41	□
Glycerol (G)	950	57	△
PG(90) + G (10)*	70	35	◑
PG(80) + G(20)	80	36	◐
PG(70) + G(30)	110	36	◓
PG(60) + G(40)	140	36	◒
PG(50) + G(50)	230	39	ⓘ
PG(40) + G(60)	310	41	⊖
PG(30) + G(70)	340	41	⊗
DG(80) + EG(20)	26	41	◨
DG(70) + EG(30)	22	42	◧
G(60) + DG(40)	230	47	◹
G(95) + Water (10)	370	60	▲

*Volume per cent of the agents is given in parentheses. The symbols listed are used in some of the figures.

3. Results and discussion

Fatigue crack growth rates, dc/dN, in air and in propylene glycol (PG) are plotted as a function of ΔK in Fig. 2, which also shows the variation of the fracture markings with the speed of crack. These data obtained at the ranges of loading frequency 0.45 to 0.8 Hz are slightly dependent on frequency. The data in the other agents almost lie on the curve tested in PG. As indicated in the figure, the dc/dN–ΔK curve may consist of two regions, i.e. Region I at relatively low values of ΔK, and Region II at high ΔK values. This trend is consistent with the result obtained by Mai [7]. In both regions, the power law relationship normally used between dc/dN and ΔK, i.e. $dc/dN = A\ (\Delta K)^n$ where A and n are constants, may be applied. In the organic agents, the exponent n is smaller in Region II than in Region I. The reverse is true in air.

The fracture surfaces tested in the organic agents, the typical features of which are nearly independent of the kind of the agents used, are very different from those in air. In air, shell-like

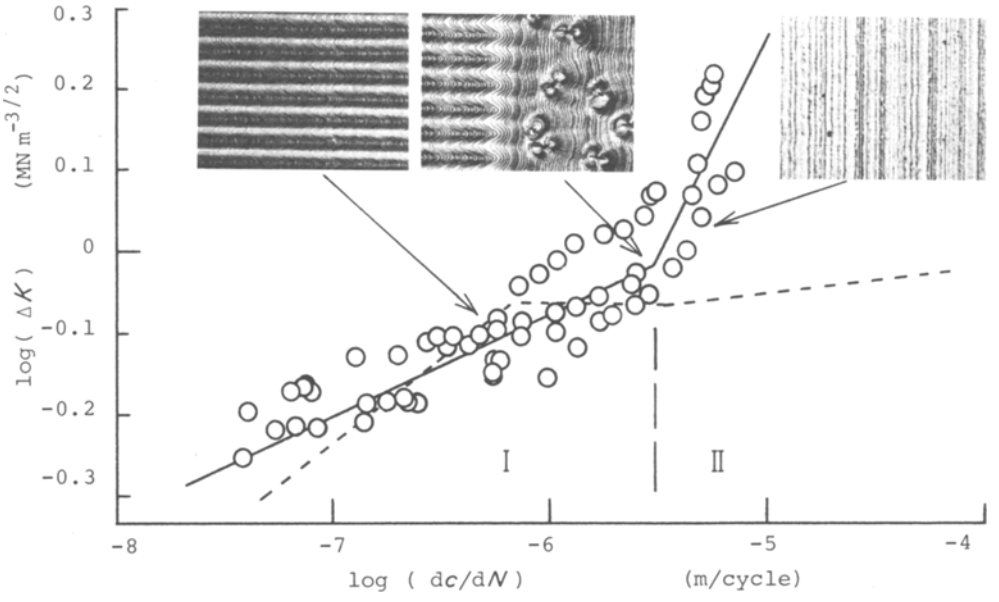

Figure 2 Crack growth rate as a function of stress intensity factor range in propylene glycol (the solid line empirically drawn through the open circles) and in air (the dotted line) and typical fracture markings at different crack speeds in the agent.

markings which include irregular fine striations and straight long-striations crossing the entire specimen thickness are obvious in Regions I and II, respectively. In the organic agents, on the other hand, regular wavy striations in Region I, bivalve shell-like markings in the transition region from Region I to II and straight long-striations in Region II are observed.

In this paper, we consider the initiation mechanism of the wavy striations in the organic agents. This may be attributed to the fluid meniscus instability observed and analysed by Pearson [8] and Pitts and Greiller [9] when films of highly viscous fluid are formed by passing the fluid through a small gap under large solid rollers. Argon and Salama [10] applied their theory to the craze initiation mechanism with success.

A schematic illustration of the fluid flow between the crack planes is shown in Fig. 3. When the applied load increases, a craze zone forms at the tip of the crack. The air shut in the polymer solid due to some forming processes will originate within the craze zone. This may be true since the bubbles of air are frequently observed through a travelling microscope in large crazes just initiated; or the air which already existed in a narrow crevice of the crack before the immersion of the test piece into the fluid will move into the craze zone. The air stored within the craze in this way is pushed out back towards the crack tip when the load decreases exceeding a maximum. The meniscus will form at the interface between the fluid and the air. The meniscus becomes unstable when the pressure gradient across it satisfies a certain condition owing to a small perturbation. As the crack closes further, the unstable flow of the fluid will be increased. When the crack opens again, the perturbed flow runs against the crack tip. Those parts of the crack tip which collide first with the disturbed flow, grow in advance of the other parts because of the environmental attack of the fluid. The repetition may cause the wavy striation.

Using the above mentioned concept, a quantitative explanation may be obtained. The analysis described below is based on the method of Pearson [8] and others [9, 10].

When the fluid flows through a gap between parallel rigid plates, the gradient of pressure is given by the equation

$$\frac{d\sigma}{dx} = 3\mu U_0/h^2 \qquad (1)$$

where Newtonian viscous flow is assumed, σ is the negative pressure, U_0 is the average velocity of the fluid, μ is the viscosity and $2h$ is the height of the gap.

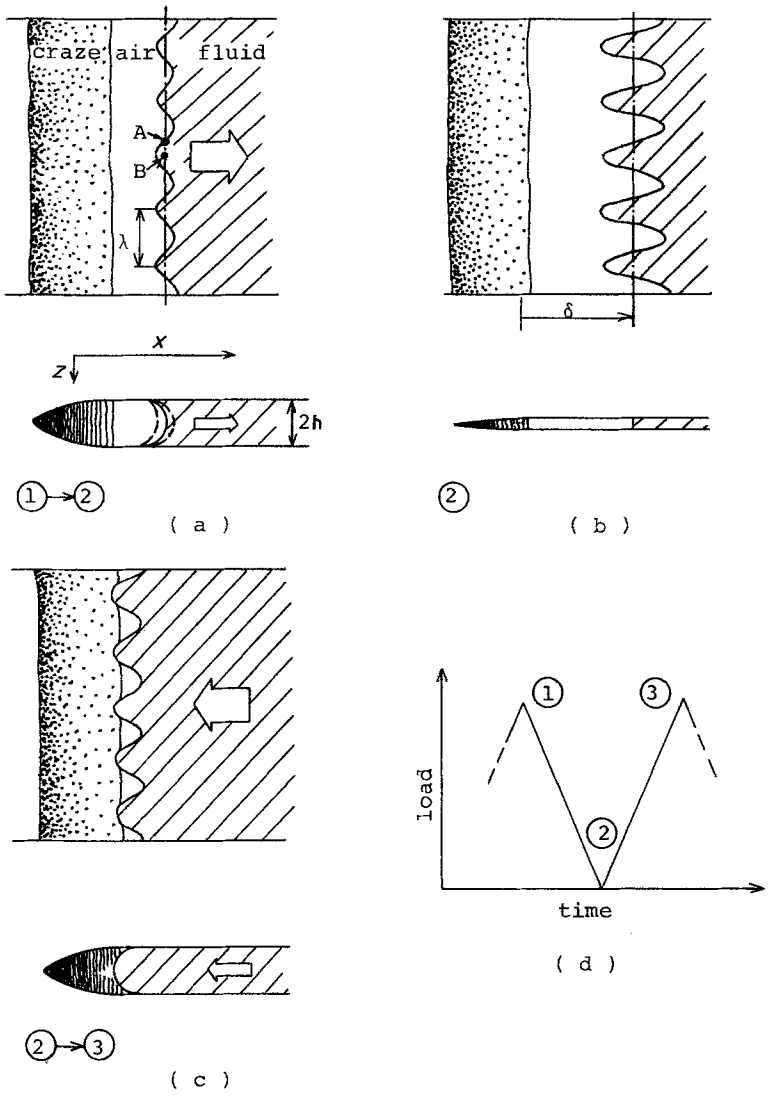

Figure 3 Initiation mechanism of wavy striation based on the meniscus instability. The large arrows show the fluid flow direction. The number in the circle shows the loading condition (*d*). (a) Initiation of meniscus instability. (b) Increase in perturbation of fluid flow. (c) Collision of fluid with craze zone. (d) Loading cycle.

Let us imagine two different points, A and B, shown in Fig. 3, owing to a small perturbation. The negative pressures, σ_A and σ_B, may be described by

$$\sigma_A = T/R \tag{2}$$

$$\sigma_B = T/R - [\mathrm{d}(T/R)/\mathrm{d}x - \mathrm{d}\sigma/\mathrm{d}x]\mathrm{d}x$$

where T is the surface tension of the fluid, R is the curvature and x is defined in the figure. If $\sigma_A < \sigma_B$, the fluid will flow in the direction from A to B. As a result, the perturbation will be increased, so that the meniscus becomes unstable. This leads to an instability condition

$$\frac{\mathrm{d}\sigma}{\mathrm{d}x} > -\frac{T}{R^2}\frac{\mathrm{d}R}{\mathrm{d}x} \tag{3}$$

The curvature R decreases with an increase in x as schematically illustrated in Fig. 3. Enormous effort will be required for the evaluation of an exact form of $\mathrm{d}R/\mathrm{d}x$. Thus, for simplicity, $-\mathrm{d}R/\mathrm{d}x$ is assumed constant. This gives a rough instability condition

$$T < C\mu f \tag{4}$$

where the fluid velocity, U_0, is assumed to be proportional to the loading frequency (see Equation 10), R^2 in Equation 3 is replaced by h^2 and C is the constant.

This shows that the air–fluid boundary will not have a wavy crest unless the viscosity μ and surface tension T of the fluid satisfy a critical condition. The fluid with low μ and high T will depress the wavy motion of the air–fluid inter-

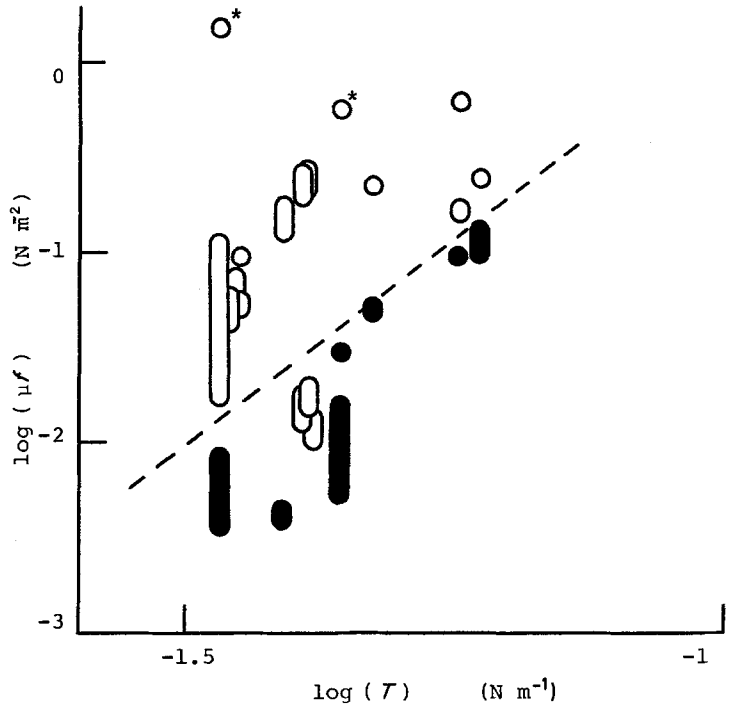

Figure 4 Critical condition for the initiation of wavy striation based on Equation 4. The solid and open marks denote the regions where the wavy striations are and are not observed, respectively. The points marked with an asterisk (*) are obtained from pure bending fatigue test.

face and the interface will become flat. In this case, therefore, straight striations as observed on the fracture surface tested in air will appear.

Although the above treatment is very simplified, it may predict the parameters which govern the initiation of the meniscus instability.

Once the meniscus instability occurs, small changes in the shape of the meniscus may be introduced. Now suppose that the meniscus cuts the x–z plane in the curve

$$x = x_0 + \varepsilon_0 e^{st} \cos mz \tag{5}$$

where ε_0 is a small length, t is the time and s and m are the constants to be determined. The perturbation produces the velocities of the fluid in the x- and z-directions described by

$$U_x = U_0(y)\,[1 + \varepsilon_0 e^{st} F(x) \cos mz] \tag{6}$$

$$U_z = U_0(y)\,\varepsilon_0 e^{st} G(x) \sin mz$$

where $U_0(y)$ is the fluid velocity described as a function of y^2 and $F(x)$ and $G(x)$ are the functions of x. Considering that the flow is two-dimensional, both the equation of force equilibrium and the equation of continuity lead to

$$F(x) = G(x) = m(1 - m^2 T/D)e^{-mx} \tag{7}$$

where $D = 3\mu U_0/h^2$. The velocity U_x in Equation 6 is equated to the time derivative of Equation 5. This gives

$$s = m\,(1 - m^2 T/D)U_0 \tag{8}$$

The fluid flow will be perturbed so that s may take a maximum with respect to m. This condition leads to the wavelength, λ,

$$\lambda = 2\pi/m = 2\pi(Th^2/\mu U_0)^{1/2} \tag{9}$$

If the fluid will move over the distance δ during the half-loading cycle, the wave form of which is triangular, the average velocity, U_0, may be written by

$$U_0 = 2f\delta \tag{10}$$

where the length δ is assumed as the region where the flow from both sides of the specimen does not occur. This length may be a function of the specimen thickness, the effect of which is not considered here. The gap $2h$ may be calculated from the theory of fracture mechanics as follows

$$h = \frac{4(1 - \nu^2)}{E} \Delta K \left(\frac{x}{2\pi}\right)^{1/2} \tag{11}$$

where E is the elastic modulus and ν is Poisson's ratio.

In the following paragraphs, a comparison of the equations mentioned above with the experimental data is made.

Fig. 4 shows the regions where the wavy

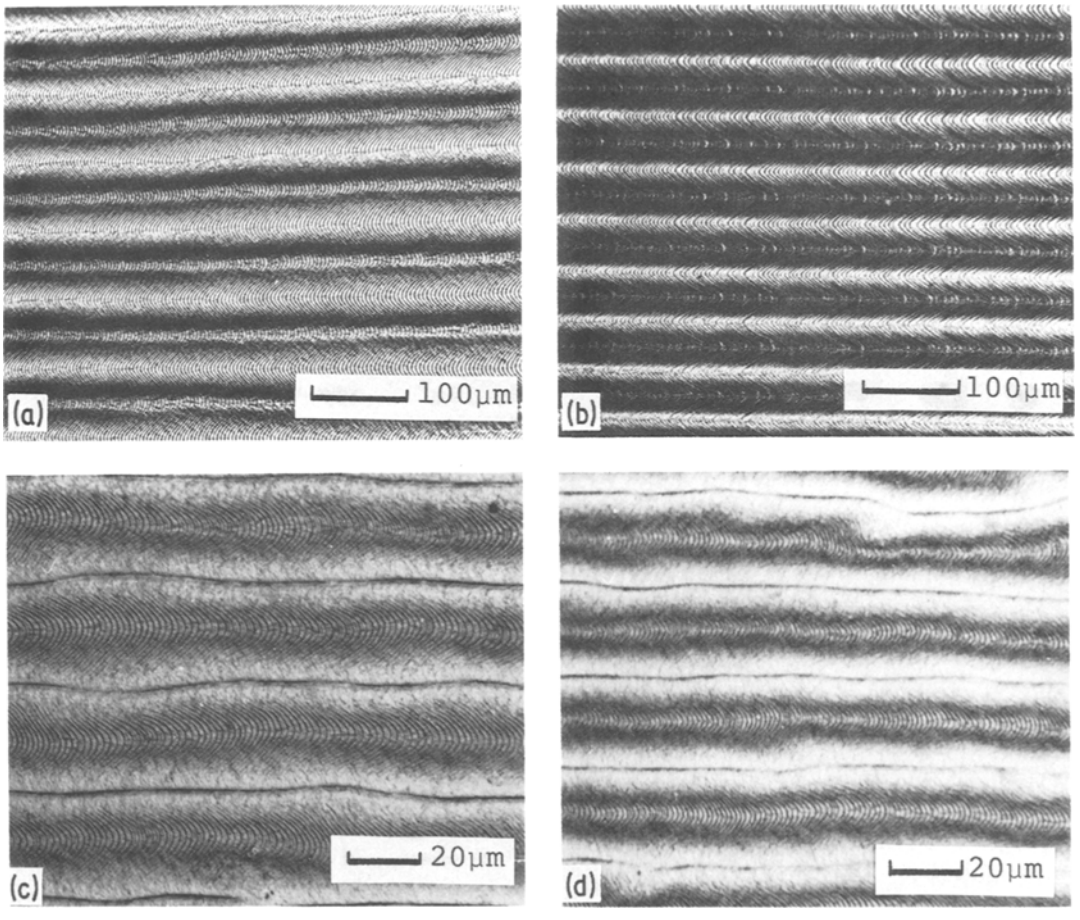

Figure 5 Wavy striations tested in various organic agents; (a) in ethylene glycol (30%) + diethylene glycol (70%); (b) in propylene glycol; (c) in propylene glycol (30%) + glycerol (70%); (d) in diethylene glycol (40%) + glycerol (60%). The crack propagates from left to right.

striations were recognized (the open marks) or not (the solid marks) for all experimental conditions adopted here. It will be seen that except for some liquids, a μf against T diagram based on Equation 4 is useful for inferring a critical condition for the initiation of the wavy striation. But, the empirical equation expressing the critical condition is of the form

$$\mu f = AT^{4.4} \ (A = \text{constant}) \qquad (12)$$

which is difficult from Equation 4. This difference may be caused by the uncertainty of the evaluation of dR/dx in Equation 3.

Fig. 5 shows the aspects of the wavy striations tested at nearly the same values of ΔK and f in the organic agents with various values of μ and T. The wavelengths measured from these photographs are plotted based on Equation 9 in Fig. 6. It is found that except for large λ, λ linearly increases with an increase in $T(\Delta K)^2/\mu f$ on a double logarithmic diagram and its slope is nearly equal to 1/2. The solid line in Fig. 6 denotes Equation 9 with the constants as follows: $E = 3500\,\text{MPa}$, $v = 0.35$, x (the half craze length) $= 1.75 \times 10^{-5}\,\text{m}$ in Equation 11 and $\delta = 1.3 \times 10^{-2}\,\text{m}$ in Equation 10. The value of x adopted here is obtained from the work of Döll *et al.* [11] who measured the craze zone length in front of the advancing crack with a variety of growth rates. The length δ, determined such that the equation may have a best fit with the experimental data, may be reasonable since it nearly corresponds to the distance over which air bubbles remaining near the crack tip move during one cycle.

To ensure this trend, pure bending fatigue tests were performed at a high loading frequency of 30 Hz using 10 mm thick specimens in contact

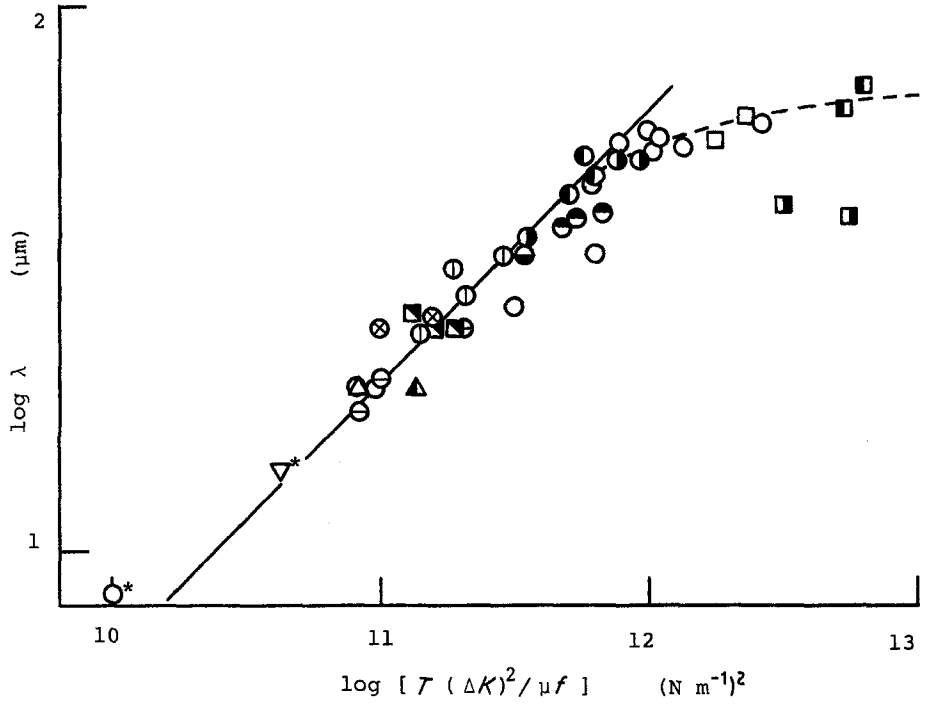

Figure 6 Wavelength, λ, as a function of the properties of the organic agent and the loading conditions. The points marked with an asterisk(*) show the data obtained from the bending fatigue test. The symbols are listed in Table I. The solid line is theoretical.

with some agents. The results are plotted by points marked with an asterisk(*) in Figs. 4 and 6.

It is shown that the experimental trend is well explained at relatively low values of λ. But at high λ values, the experimental data (the dotted curve in Fig. 6) somewhat depart from Equation 10, and may indicate that the wavelength, λ, is not able to exceed a certain critical level independent of the kind of environmental agents. A probable reason for this departure remains vague.

The other features of the wavy striations are discussed. Fig. 7 shows the relationship between the spacing of the wavy striation and the macroscopic crack growth rate. It will be seen that the striations form during each load excursion. In this sense, they are not different from the usually observed ones in various kinds of polymers. Fig. 8 shows the relationship between the wavelength, λ, and its amplitude, ε, corresponding to $\varepsilon_0 e^{st}$ in Equation 6. It is found that ε is nearly proportional to λ, i.e. $\varepsilon = 0.3\lambda$. The theoretical analysis described here unfortunately may not provide a means to estimate the magnitude of ε quantitatively.

From Fig. 5, it will be seen that the surface is three-dimensional, that is, it is regularly convex and concave to it and the crack goes ahead at the concave parts rather than at the convex ones. The concave and convex parts on both fracture surfaces match each other and make a number of channels, through which the fluid flow becomes more easy. Once the channels form due to the meniscus instability, the wavy striations probably continue to initiate readily.

When the crack growth rate exceeds a certain value slightly dependent on the environmental agent, bivalve-shell like markings, an enlargement of which is shown in Fig. 9, suddenly appear on the fracture surface in place of the wavy striations. In this region (Region II) where ΔK is relatively high, the craze zone is clearly observed ahead of the crack, even by the unaided eyes, and is considerably longer than in Region I. This sudden change in the craze zone length may effect the fluid flow so that its tips may go round into the fibrils of crazes. This makes large voids due to the environmental attack, and then striations develop around the voids. These processes may give the bivalve-shell like markings. The density, ϱ, of the bivalve shell

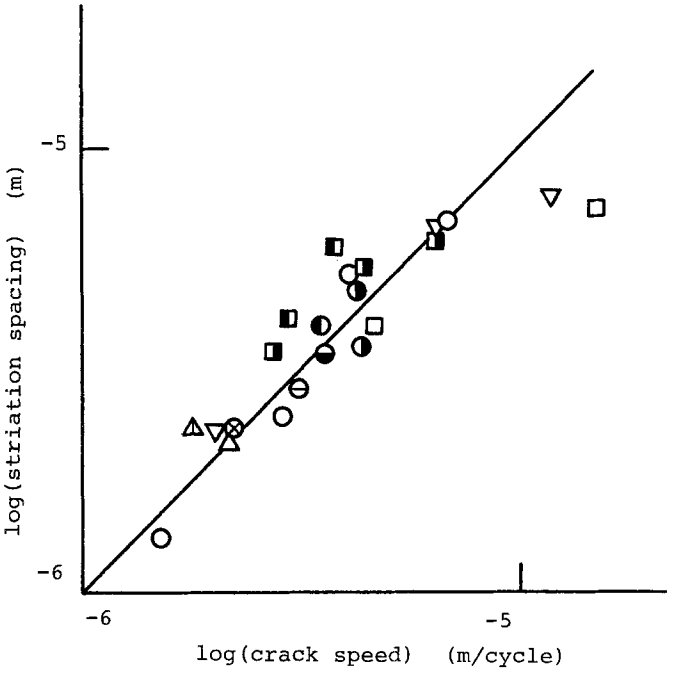

Figure 7 Relationship between macroscopic crack speed and striation spacing. The symbols are denoted in Table I.

markings at the transition region from I to II is plotted against the wavelength in Fig. 10. This indicates that as λ becomes small, ϱ abruptly increases in obedience to $\varrho \propto \lambda^{-2}$. Further increase in the crack speed decreases ϱ, and at last, long striations crossing the entire specimen thickness cover the fracture surface.

The above discussion may show that the wavy striation forms due to the meniscus instability of the fluid which penetrates into the crack. But in this paper, evidence that the meniscus can be constructed near the crack tip was not verified from observation through an optical microscope. Further work will be needed.

4. Conclusions

Fatigue tests of PMMA plates were carried out in organic agents with relatively high viscosity. New type striations were observed on the fracture surface. These striations, which formed at relatively low values of ΔK, i.e. at low cracking speeds up to about 10^{-5} m/cycle, were regularly

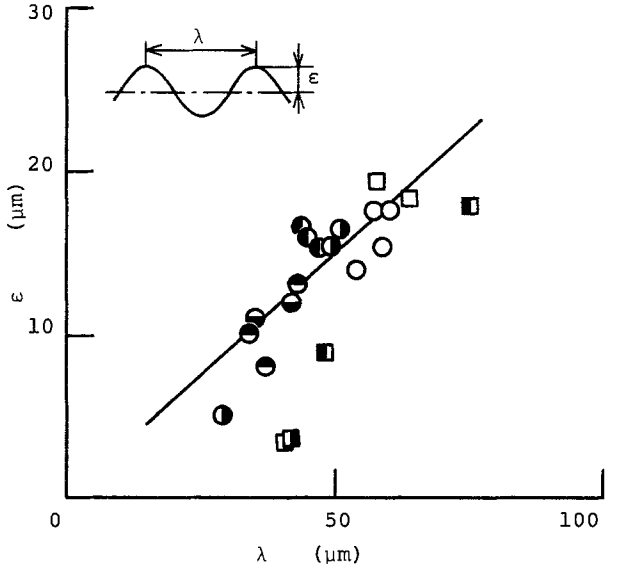

Figure 8 Variation of amplitude of wavy striation, ε, with its wavelength, λ. The symbols are shown in Table I.

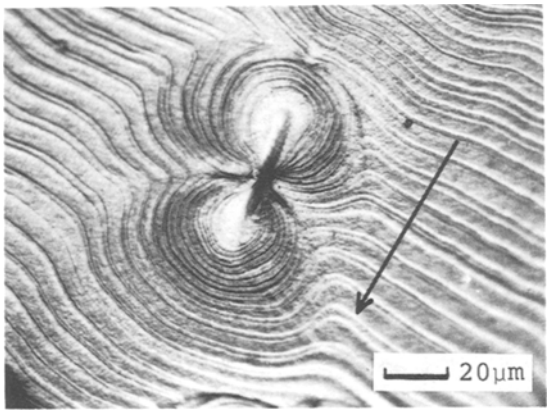

Figure 9 Enlargement of bivalve shell-like marking. The arrow shows the crack growth direction.

wavy. A theoretical analysis is done on the basis of the assumption that these will form due to the instability of the meniscus initiated at the interface of the viscous fluid with the air left within the craze zone at the crack tip. The theory suggests that the wavelength of the striation is determined by the characteristics of the organic agent, such as viscosity and surface tension, and the loading conditions, such as stress intensity factor range and loading frequency (see Equation 10). This suggestion was in good agreement with the experimental trend at low values of the wavelength.

In this paper, the wavy striations were investigated using only one kind of glassy polymer. Whether or not these form in the other polymers was not tested. Furthermore, the formation of the meniscus, which is the foundation of the theory, was not verified by means of the present observation. Further work will be required.

Acknowledgement

The authors wish to thank Mr H. Asano for his technical assistance.

References

1. G. P. MARSHALL, L. E. CULVER and J. G. WILLIAMS, *Plastics & Polymers* **37** (1969) 75.
2. J. G. WILLIAMS and G. P. MARSHALL, *Proc. Roy. Soc. Lond.* **A342** (1975) 55.
3. A. G. ATKINS, C. S. LEE and R. M. CADDEL, *J. Mater. Sci.* **10** (1975) 1381.
4. B. MUKHERJEE, L. E. CULVER and D. J. BURNS, D. J. BURNS, *Exp. Mech.* **9** (1969) 90.
5. R. W. HERTZBERG, M. D. SKIBO and J. A. MANSON, *J. Mater. Sci.* **13** (1978) 1038.
6. ASTM Standard E399-72, (American Society for Testing and Materials, Philadelphia, 1972).
7. Y. W. MAI, *J. Mater. Sci.* **9** (1974) 1896.
8. J. R. A. PEARSON, *J. Fluid Mech.* **7** (1960) 480.
9. E. PITTS and J. GREILLER, *ibid.* **11** (1961) 33.
10. A. S. ARGON and M. SALAMA, *Mater. Sci. Eng.* **23** (1976) 219.
11. W. DÖLL, M. G. SCHINKER and L. KOENCZOEL, *Int. J. Fracture* **15** (1979) R145.

Received 3 February
and accepted 30 April 1984

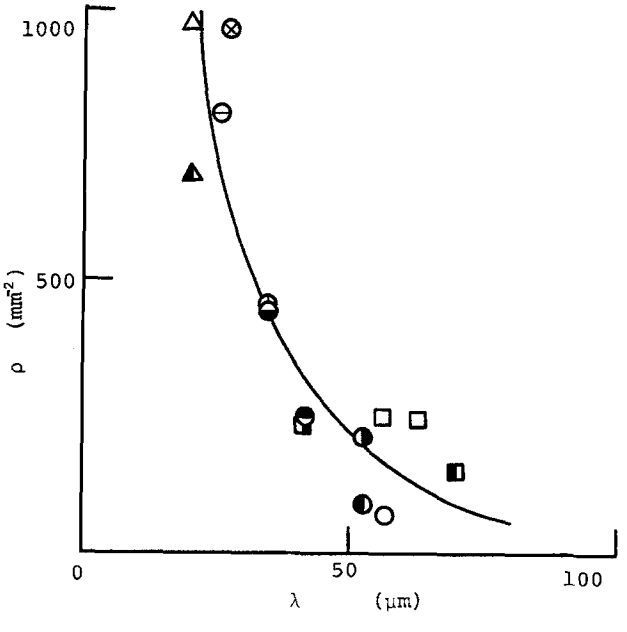

Figure 10 Variation of the density, ϱ, of bivalve shell marking with wavelength, λ. The symbols are denoted in Table I.